TISSUE ENGINEERING: Part A
Volume 16, Number 12, 2010
© Mary Ann Liebert, Inc.
DOI: 10.1089/ten.tea.2009.0837

Biomimetic Microenvironment Modulates Neural Stem Cell Survival, Migration, and Differentiation

Sarah E. Stabenfeldt, Ph.D.,[1] Gautam Munglani, B.S.,[1]
Andrés J. García, Ph.D.,[2] and Michelle C. LaPlaca, Ph.D.[1]

Biomaterial matrices presenting extracellular matrix (ECM) components in a controlled three-dimensional configuration provide a unique system to study neural stem cell (NSC)–ECM interactions. We cultured primary murine neurospheres in a methylcellulose (MC) scaffold functionalized with laminin-1 (MC-x-LN1) and monitored NSC survival, apoptosis, migration, differentiation, and matrix production. Overall, MC-x-LN1 enhanced both NSC survival and maturation compared with MC controls. Significantly lower levels of apoptotic activity were observed in MC-x-LN1 than in MC controls, as measured by *bcl-2/bax* gene expression and tetramethylrhodamine-dUTP nick end labeling. A higher percentage of NSCs extended neurites in a β_1-integrin-mediated fashion in MC-x-LN1 than in MC controls. Further, the differentiation profiles of NSCs in MC-x-LN1 exhibited higher levels of neuronal and oligodendrocyte precursor markers than in MC controls. LN1 production and co-localization with $\alpha_6\beta_1$ integrins was markedly increased within MC-x-LN1, whereas the production of fibronectin was more pronounced in MC controls. These findings demonstrate that NSC microenvironments modulate cellular activity throughout the neurosphere, contributing to our understanding of ECM-mediated NSC behavior and provide new avenues for developing rationally designed couriers for neurotransplantation.

Introduction

A highly organized cellular microenvironment, including a unique assembly of extracellular matrix (ECM) proteins, is critical to cellular development.[1] Neural stem cells (NSCs) derived from the developing germinal eminence present an attractive model to study cell–ECM interactions associated with neural development and also for developing regenerative biomaterial systems that incorporate ECM support.[2] NSCs cultures are often maintained as proliferative neurospheres and give rise to multiple cell types (i.e., neuronal, astrocyte, and oligodendrocyte lineages) in response to defined cues.[2]

ECM–integrin interactions are fundamental to NSC survival, proliferation, differentiation, and migration.[3–5] NSCs within the developing germinal eminence express α_6 and β_1 integrin receptors co-localized with laminin (LN) chains,[6] an interaction that remains prominent in the ventricular NSC niche throughout adulthood.[7] Additionally, NSCs cultured as neurospheres *in vitro* produce multiple isoforms of LN and β_1 integrins.[6] In the absence of β_1 integrin signaling, NSC neurospheres undergo apoptosis.[3] When exposed to exogenous fibronectin (FN) or laminin-1 (LN1) adsorbed on a two-dimensional (2D) substrate, cellular migration from the neurosphere is partially mediated through β_1 integrins.[3–5] NSCs plated on LN1 exhibit a more mature neuronal profile than FN or collagen IV substrates.[4] Collectively, these observations underscore the important role ECM–cell interactions play within the stem cell niche for neural survival and differentiation.

Synthetic scaffolds have been used to investigate NSC responses to soluble and/or immobilized ligands on both 2D and three-dimensional (3D) substrates.[8–10] Ligands tethered to a 3D matrix provide more *in vivo*-like cell–ECM interactions than 2D counterparts.[11,12] Here, we utilize methylcellulose (MC) as a polymeric foundation to evaluate the effect of 3D LN1 presentation on NSC behavior. MC is a temperature-sensitive polymer used in several neural tissue engineering applications.[13–16] Tethering LN1 to MC enables examination of NSC–LN1 interactions in a controlled 3D configuration, as the low levels of protein adsorption onto MC minimize non-specific cellular binding.[13] Additionally, MC tethered to LN1 generates a potential delivery vehicle for neural transplantation that may address current limitations such as poor donor cell survival.[17] Co-delivery of NSCs with pro-survival cues, such as LN1, may therefore prevent and/or reduce apoptosis,

[1]Laboratory for Neuroengineering, Coulter Department of Biomedical Engineering, Petit Institute for Bioengineering and Bioscience, Georgia Institute of Technology, Emory University, Atlanta, Georgia.
[2]Petit Institute for Bioengineering and Bioscience, Georgia Institute of Technology, Woodruff School of Mechanical Engineering, Atlanta, Georgia.

thereby improving transplant survival while presenting both migration and differentiation cues to donor cells.[18–21]

In this study, we evaluated the influence of a 3D LN1 microenvironment on multiple aspects of NSC behavior. We hypothesized that NSC-derived neurospheres cultured within an exogenous LN1 milieu will survive, migrate from the neurosphere, and differentiate to a greater extent than those cultured in MC alone. Foremost, we expected that the presence of exogenous LN1 would enable the cell population at the periphery of the sphere to possess a higher percentage of committed cells, leading to an increased propensity to migrate out of the sphere.

Methods

NSC harvest and culture

Colony breeding and harvest procedures were approved by the Institutional Animal Care and Use Committee of the Georgia Institute of Technology. NSC neurospheres were obtained from fetal transgenic C57BL/6-Tg(CAG-EGFP)C14-Y01-FM131Osb mice.[4,22] Briefly, pregnant mice (gestational day 14.5) were anesthetized with isoflurane and sacrificed. The fetuses were isolated by Caesarian section and decapitated. Upon removal of the skull, parasagittal cuts were made in each hemisphere. The lateral ganglonic eminence was isolated from underlying tissue and mechanically dissociated in Hank's balanced salt solution (Invitrogen). Dissociated cells were plated and maintained as suspension cultures in uncoated T-25 vented culture flasks at 37°C, 5% CO_2, and 95% relative humidity in NSC medium–serum-free Dulbecco's modified Eagle's medium/F12 (Invitrogen) supplemented with insulin (25 μg/mL), transferrin (100 μg/mL), putrescine (60 μM), sodium selenite (30 nM), progesterone (20 nM), and glucose (6 μg/mL). Human recombinant basic fibroblast growth factor (bFGF, 20 ng/mL; Peprotech) supplements were added every other day to maintain proliferation. The NSC cultures formed suspended neurospheres over 7–10 days at which point the neurospheres were dissociated into a single cell suspension and split at 1:3 ratio into new culture flasks. All experimental assays were performed with NSC neurospheres of passage 3–5. By isolating NSCs from the transgenic mouse mice expressing green fluorescent protein (GFP) driven by a β-actin promoter, NSC viability, migration, and neurite outgrowth can be monitored in real-time. All reagents were obtained from Sigma-Aldrich unless indicated otherwise.

Tethering of LN1 to MC

MC ($M_w \sim 40$ kDa) hydrogels were prepared in Dulbecco's phosphate-buffered saline (DPBS; Invitrogen) using a dispersion technique.[13,23] The photocrosslinker *N*-sulfosuccinimidyl-6-[4′-azido-2′-nitrophenylamino] hexanoate (sulfo-SANPAH; Pierce Biotechnology; Fig. 1) was used to tethering LN1 to MC. LN1 (200 μg/mL; Invitrogen) was incubated with sulfo-SANPAH solution (0.5 mg/mL) in the dark for 2.5 h. Residual unreacted sulfo-SANPAH was removed with microcentrifuge filters. LN1-SANPAH (200 μg/mL) was reconstituted and thoroughly mixed on ice with MC (7.2% w/v). A thin layer (~150 μm) of the MC+LN1-SANPAH mixture was then cast onto a glass slide and exposed to UV light for 4 min (100W, 365 nm; BP-100AP lamp; UVP), initiating the photocrosslinking reaction. Upon completion of the tethering reaction, unbound LN1 was removed by rinsing with DPBS plus 0.1% Tween-20 then DPBS alone. MC tethered to LN1 is referred to as MC-x-LN1. Controls included bovine serum albumin (BSA) tethered to MC (MC-x-BSA) and MC supplemented with soluble LN1 (MC+LN1) to account for residual nontethered LN1 trapped within MC. LN1 tethering density of the end reaction product was quantified with a dot blot and image analysis of intensity per area measurements (Multi-Gauge Analysis software; Fujifilm). This assay determined the amount of LN1 that was incorporated into the MC as a result of the tethering reaction and does not reveal any information about distribution of LN1 when the cells are cast with the hydrogels, as no cells were present at this stage.

3D NSC cultures within MC

NSC neurospheres (passages 3–5) were suspended in NSC medium and mixed with MC at a 1:5 ratio (final seeding density of 5×10^6 cells/mL of MC). The cell-MC solution was dispensed into small chambers (5 mm in diameter) on coverglass to obtain a 300 μm thick hydrogel. The plated cell-MC solution was allowed to gel at 37°C for 45 min and then NSC medium was added. For all experimental groups (MC-x-BSA, MC+LN1, and MC-x-LN1), bFGF was absent. The control groups included NSCs plated on LN1-coated polystyrene (5 μg/cm^2; seeding density 5×10^5 cells/cm^2) and NSCs cultured in suspension with and without bFGF. All cultures were maintained in a tissue culture incubator with media exchanges every other day until performing a predetermined endpoint assay (see subsequent methods for endpoint assays).

Cell viability

Release of lactic dehydrogenase (LDH) into the cell medium is an indicator of compromised cellular membranes and thus an indirect measure of cell death.[24] This assay served as an initial screening tool to detect cell death. At 2, 4, and 7 days, 50 μL of NSC medium from atop of the MC 3D cultures was collected and the LDH content measured (*In Vitro* Toxicology Assay Kit; $n = 3$–4 trials in triplicate per group). Samples were transferred to a 96-well plate and mixed with 100 μL of LDH reagent solution. After incubation (30 min at 37°C), the reaction was stopped with 15 μL of 1.0N HCL. Absorbance was measured at 490 nm. LDH levels were normalized to a LDH standard curve.

At 2, 4, and 7 days in culture, viability was also assessed by ethidium homodimer (EthD-1; Invitrogen) staining and GFP intensity; the transgenic GFP was driven by a β-actin promoter; therefore, production of GFP diminished with cell death.[25] At the specified endpoints, cell–hydrogel constructs were rinsed with DPBS and incubated a 4.0 μM EthD-1 at 37°C for 30 min. Before imaging, the stain was removed and the cultures were rinsed with DPBS. For each sample ($n = 3$–4 cultures per group), 200-μm-thick *z*-stack images were acquired at three different XY positions in the culture (Confocal Model LSM 510; Ziess), to corroborate the quantitative analysis of the LDH assay.

Apoptosis and apoptotic signaling

Quantitative reverse transcriptase polymerase chain reaction. Transcript levels of bcl-2 and bax was determined at

7 days postplating by performing quantitative reverse transcriptase-polymerase chain reaction with SYBR Green intercalating dye using the ABI Prism 7700 Sequence Detection System (Applied Biosystems; 40 cycles; melting, 15 s at 95°C; annealing and extension, 60 s at 60°C; $n = 6$–8 samples per group).[26] RNA was isolated and cDNA synthesized on DNaseI-treated total RNA by oligo(dT) priming using the Superscript First Strand Synthesis System (Invitrogen). Sequences for *bax* and *bcl-2* oligonucleotide primers were previously published[27]—*bax*: forward 5′ ATGCGTCCACCA AGAAGCTGA 3′ and reverse 5′ AGCAATCATCCTCTGCA GCTCC 3′; *bcl-2*: forward 5′ TTCGCAGCGATGTCCAGTC AGCT 3′ and reverse 5′ TGAAGAGTTCTTCCACCACCGT 3′. β-Actin expression was measured as a housekeeping control. Primer specificity was confirmed with ABI Prism 7700 Dissociation Curve Software. Standards for each gene were from cDNA using real-time oligonucleotides, purified using a Qiagen PCR Purification kit (Qiagen), and diluted over a functional concentration range. Transcript levels in template cDNA solutions were quantified from a linear standard curve and normalized to 1 μg of total RNA.

Tetramethylrhodamine-dUTP nick end labeling. Terminal deoxynucleotidyl transferase tetramethylrhodamine-dUTP nick end labeling (TUNEL) (*In Situ* Cell Death Kit, TMR; Roche Applied Science) was used to indicate apoptosis. At 7 days postplating, NSCs cultured in MC samples were rinsed with PBS, fixed with 3.7% formaldehyde for 30 min, rinsed again, embedded in OCT Compound, and then snap-frozen. Frozen cultures were cryosectioned at 15 μm and collected onto subbed (gelatin) glass slides (Microm Cryo-Star HM 560 MV Cryostat). Before TUNEL, sections were permeablized with 0.1% Triton X-100 in 0.1% sodium citrate for 30 min at room temperature. Image acquisition and analysis was performed with an LSM confocal microscope. For each group, $n = 4$–6 samples (5–8 neurospheres per sample) were quantified.

Migration and neurite outgrowth

NSCs were harvested from transgenic mice that constitutively express GFP driven by a β-actin promoter, enabling the observation of migration and outgrowth from neurospheres into the surrounding MC hydrogel. At 2, 4, and 7 days cultures, confocal microscopy z-stacks were collected with low power laser excitation for each 3D culture condition (MC-x-BSA, MC+LN1, and MC-x-LN1). Two-dimensional projections from each confocal z-stack were used to analyze migration area defined as total area of sphere normalized to an inner circular area (Fig. 4A; Image Pro-Plus Software; $n = 10$–25 per culture). For neurite outgrowth analysis, the 3D z-stack micrographs were used to quantify the number of extensions (>50 μm) protruding from GFP-positive neurospheres.

β_1 integrin blocking. NSC cultures were cultured with β_1 integrin function blocking antibodies to evaluate the role of integrin-mediated adhesion on migration and outgrowth. Experimental treatment groups ($n = 3$ cultures per group) received NSC media supplemented with anti-rat CD29 (250 μg/mL; BD Pharmingen). Control groups consisted of media only ($n = 3$ cultures) and media plus IgG isotype control (250 μg/mL; BD Pharmingen; $n = 3$ cultures). At 2, 4, and 7 days, neurite outgrowth was evaluated as described above.

Differentiation and ECM and integrin production

Immunocytochemistry was employed to examine differentiation markers and ECM production after 7 days in culture. Cryosections (15 μm thick) of MC hydrogel cultures, prepared as described above for TUNEL staining, were blocked and permeablized with a 4% goat serum solution supplemented with 0.1% Triton-X100 at room temperature for 1 h. Primary antibodies for nestin (1:100; Promega), glial fibrillary acidic protein (GFAP, 1:100; Millipore), β-tubulin III (1:1000; Covance), oligodendrocyte marker O4 (O4, 1:100; Millipore), LN1 (1:50; Sigma), FN (1:100; Millipore), integrin $\alpha_5\beta_1$ (1:50; Millipore), or integrin α_6 (1:50; Millipore) were diluted in 4% goat serum and incubated with the cyrosections for 2 h at 37°C. Sections were rinsed thrice with PBS followed by a 2 h incubation at room temperature with secondary antibodies conjugated to Alexa 546 nm or Alexa 633 nm (Invitrogen). Secondary antibody controls for each immunocytochemistry run were used to control for nonspecific binding and false-positive signal. After rinsing with PBS, sections were mounted with Fluoromount-G aqueous mounting medium, and coverslipped, and z-stack images for 2 μm slices were captured and analyzed on a LSM confocal microscope ($n = 5$–8 GFP-positive neurospheres per immunostain per group). During this protocol, residual MC-x-LN1 was rinsed from the slide as confirmed by running control sections of MC-x-LN1 only, in which minimal positive LN1 stain was observed. A blinded observer rated each confocal micrograph with a relative intensity scale ranging from negative immunostaining (–) to high positive immunostaining (+++).[28]

ECM and integrin immunocytochemistry analysis. To evaluate the spatial distribution of integrins ($\alpha_5\beta_1$ and $\alpha_6\beta1$) and FN and LN1 deposition, we developed a MATLAB program to measure the relative staining intensity of immunostained cryosections ($n = 8$–15 GFP-positive neurospheres per MC group). Previous studies have used similar methods to evaluate ECM production across spheroid cell cultures.[29] From this analysis, we generated pixel intensity maps for each immunostain and calculated the relative area of positive immunostaining. Baseline intensity levels for all samples were normalized to secondary antibody-only controls. The positive staining area was determined by normalizing the immunopositive area to the total area of the neurosphere.

Statistical analysis

Data are presented as mean ± one standard deviation. Results were analyzed by *t*-test, one-way analysis of variance (ANOVA) followed by Tukey's pairwise *post-hoc*, or two-way ANOVA followed by Bonferroni posttest. A 95% confidence level and corresponding p-value < 0.05 was considered significant. A nonparametric Kruskal–Wallis one-way ANOVA on Ranks was performed on the immunostaining scores followed by pairwise comparisons with Dunn's Method. A 95% confidence level and

corresponding p-value < 0.05 was considered significant. All statistical analyses were performed with SigmaStat software (Systat Software, Inc.).

Results

Tethered LN1 enhances NSC survival in a 3D synthetic microenvironment

LN1 was covalently linked to MC via the heterobifunctional photo-crosslinker sulfo-SANPAH. The NHS esters of sulfo-SANPAH react with primary amine groups on LN1 (Fig. 1A). Subsequent mixing of this conjugate with MC and UV irradiation converts nitrophenyl azide groups on SANPAH to nitrene groups, which then inserts into C-H bonds on MC. Tethered LN1 densities were $8.2 \pm 1.3\,\mu g$ LN1/mL of MC as determined by dot blotting (Fig. 1B), whereas MC+LN1 hydrogels contained significantly less at $0.7 \pm 0.4\,\mu g$ LN1/mL of MC ($p < 0.05$; t-test).

LDH release from the NSCs in the MC cultures was evaluated as an indirect measure of cell viability. For this assay, we compared NSCs cultured within MC-x-LN1 to cells embedded in unfunctionalized (nonadhesive) MC hydrogels (i.e., MC-x-BSA and MC+LN1). Since released LDH levels may not scale with cell seeding density, a comparison of 2D control cultures (i.e., 2D LN1-coated plates) was not included. At 2 days postplating, significantly lower LDH release was observed with NSCs cultured within MC-x-LN1 compared with MC-x-BSA ($p < 0.001$) and MC+LN1 ($p < 0.05$; Fig. 2A) ($F(2,14) = 52.205$, one-way ANOVA). MC-x-LN1 cultures maintained significantly higher viability at 4 and 7 days *in vitro* than MC-x-BSA and MC+LN1 ($p < 0.001$; $F(2,14) = 160.407$ and $F(2,14) = 46.934$, respectively, one-way ANOVA); thus, the density and/or presentation (i.e., soluble vs. tethered) of ligand influences NSC survival. Qualitative analysis with EthD-1 staining and GFP intensity corroborated the LDH assay. The representative confocal micrograph projections (Fig. 2B–J) show increased EthD-1 uptake in the MC-x-BSA and MC+LN1 groups compared with MC-x-LN1 over 7 days *in vitro*. Conversely, GFP intensity was most prominent in MC-x-LN1 cultures, providing additional evidence of preserved NSC survival.[25] Collectively, these results demonstrate the critical need to present immobilized ECM to prevent cell death.

MC-x-LN1 reduced apoptosis

Consistent with the cell survival results, apoptotic activity measured by bcl-2/bax gene expression levels (mitochondrial apoptosis pathway) and a TUNEL assay further supported the hypothesis that 3D presentation of tethered LN1 provides pro-survival signals to NSCs. At 7 days *in vitro*, quantitative reverse transcriptase-polymerase chain reaction was used to measure expression of bcl-2 (anti-apoptotic) and bax (pro-apoptotic) signaling molecules. The ratio of these molecules is indicative of the apoptotic state of the cell; lower bcl-2/bax ratios indicate higher levels of bax than bcl-2, driving the cell into an apoptotic state.[30] The

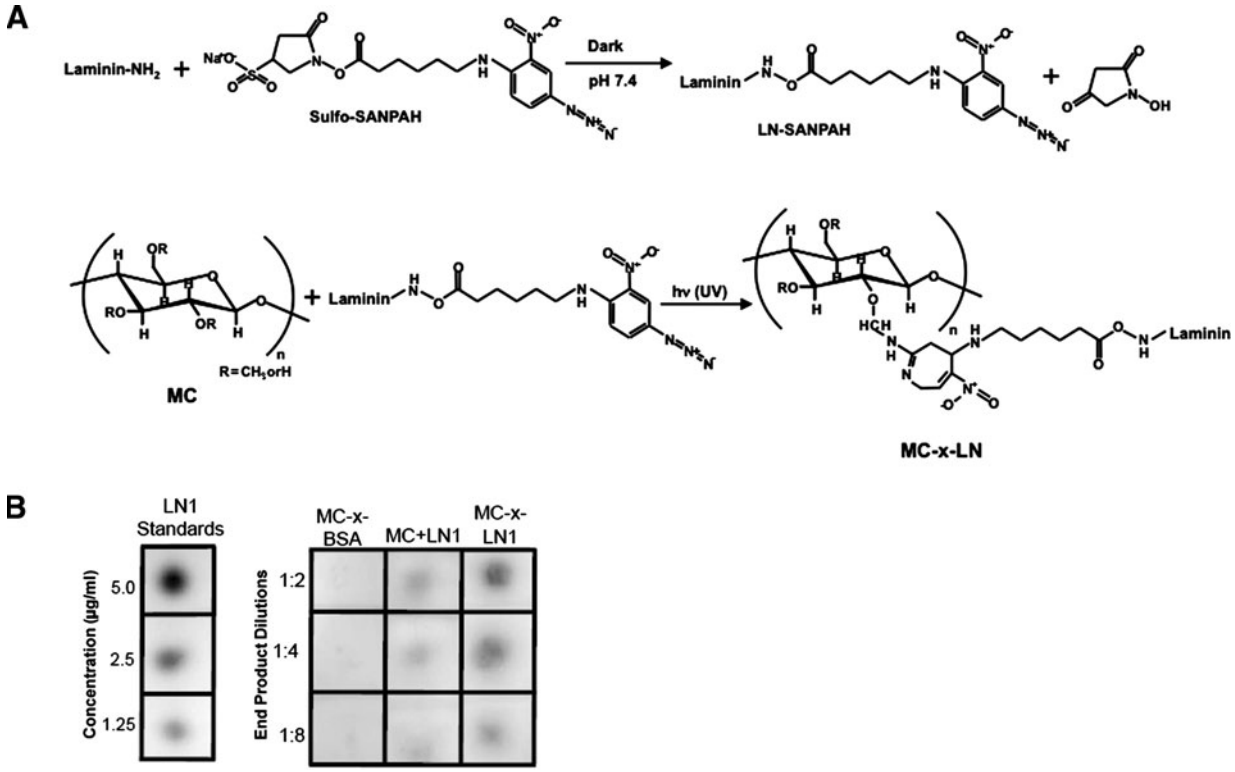

FIG. 1. MC-x-LN1 characterization. **(A)** Tethering scheme: NHS ester groups on sulfo-SANPAH react with primary amino groups on LN1 to form stable amide bonds. Subsequent mixing with MC in addition to UV irradiation initiated the formation of a nitrene group which inserts into C-H bonds on MC. **(B)** Quantitative dot blots measured the LN1 density for the final reaction products. The density for MC-x-LN1 was $8.2 \pm 1.3\,\mu g$ LN1/mL of MC and MC+LN1 was $0.7 \pm 0.4\,\mu g$/mL. MC, methylcellulose; LN1, laminin-1.

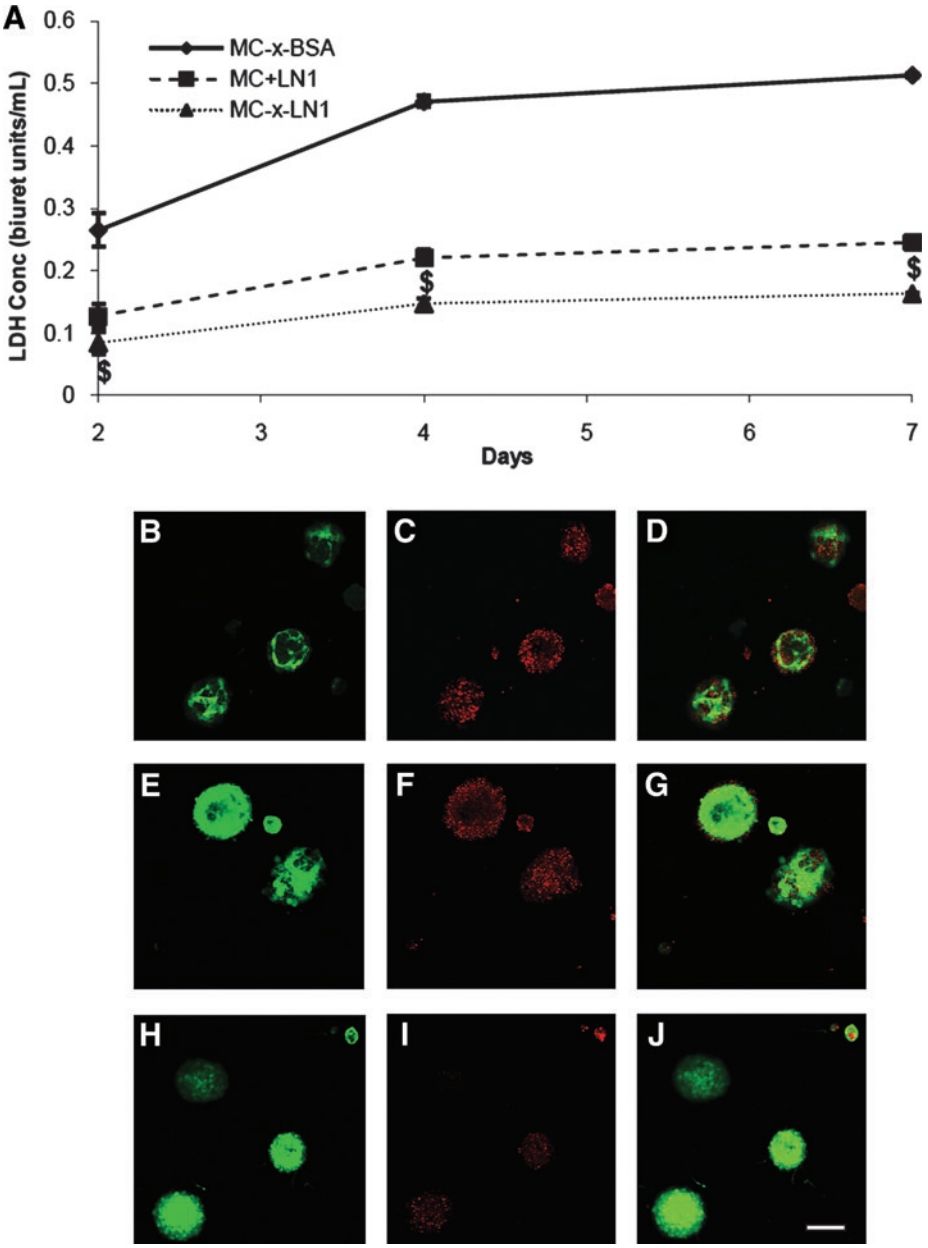

FIG. 2. NSC viability is supported in MC-x-LN1. **(A)** Over 7 days, NSCs cultured within MC-x-LN1 had significantly lower levels of LDH release than MC controls ($^{\$}p < 0.05$). **(B–J)** Confocal micrograph 5 μm slice from the 200μm z-stacks at 7 days postplating of GFP on actin promoter (green; **B, E, H**), EthD-1 (red; **C, F, I**), and merged GFP and EthD-1 **(D, G, J)**. EthD-1 uptake was highest for NSCs plated within MC-x-BSA (**C** and **D**), decreased with MC+LN1 (**F** and **G**), and lowest within MC-x-LN1 (**I** and **J**). Scale bar 100 μm. BSA, bovine serum albumin; GFP, green fluorescent protein; EthD-1, ethidium homodimer; LDH, lactic dehydrogenase; NSC, neural stem cell. Color images available online at www.liebertonline.com/ten.

ratio of bcl-2 to bax levels was significantly higher in MC-x-LN1 than in all groups, including the 2D LN1 control (Fig. 3A) ($p < 0.05$; $F(3,19) = 17.72$, one-way ANOVA). TUNEL was then used to identify fragmented DNA. The micrographs in Figure 3C–F are representative TUNEL images for the MC groups and a 2D LN1-positive reference. At 7 days postplating, significantly fewer TUNEL$^+$ cells were observed in MC-x-LN1 (30%) than in MC-x-BSA (65%) and MC+LN1 (57%; Fig. 3B) ($p < 0.05$; $F(3,19) = 12.013$, one-way ANOVA). Similarly, 2D LN1-coated positive control substrates contained few TUNEL$^+$ NSCs, indicating the pro-survival capacity of LN1.

Neurite outgrowth, but not migration, is enhanced in MC-x-LN1

LN1 stimulates migration and outgrowth from NSC neurospheres.[4] Therefore, we measured both the migration and neurite outgrowth from neurospheres within a 3D environment as a function of LN1 presentation. We defined migration as the total area of the neurosphere normalized to the largest inner circle (Fig. 4A). At 7 days *in vitro*, migration from the viable neurospheres significantly increased when LN1 was present in either MC+LN1 or MC-x-LN1 compared with MC-x-BSA (Fig. 4B). However, no migration difference was observed between MC+LN1 and MC-x-LN1. In addition to migration, we quantified the percentage of neurospheres extending projections. Within the 3D MC groups, we observed significant outgrowth in the MC-x-LN1 cultures compared with MC-x-BSA and MC+LN1 at 4 and 7 days (Fig. 4C) ($p < 0.001$, $F(2,72) = 86.43$ for MC formulation, two-way ANOVA). Importantly, the addition of a function-perturbing β_1 integrin antibody significantly blocked outgrowth in MC-x-LN1 at all time points and MC+LN1 at 4 days (Fig. 4D) ($p < 0.05$, $F(5,144) = 92.17$ for MC formulation, two-way ANOVA), suggesting that NSC

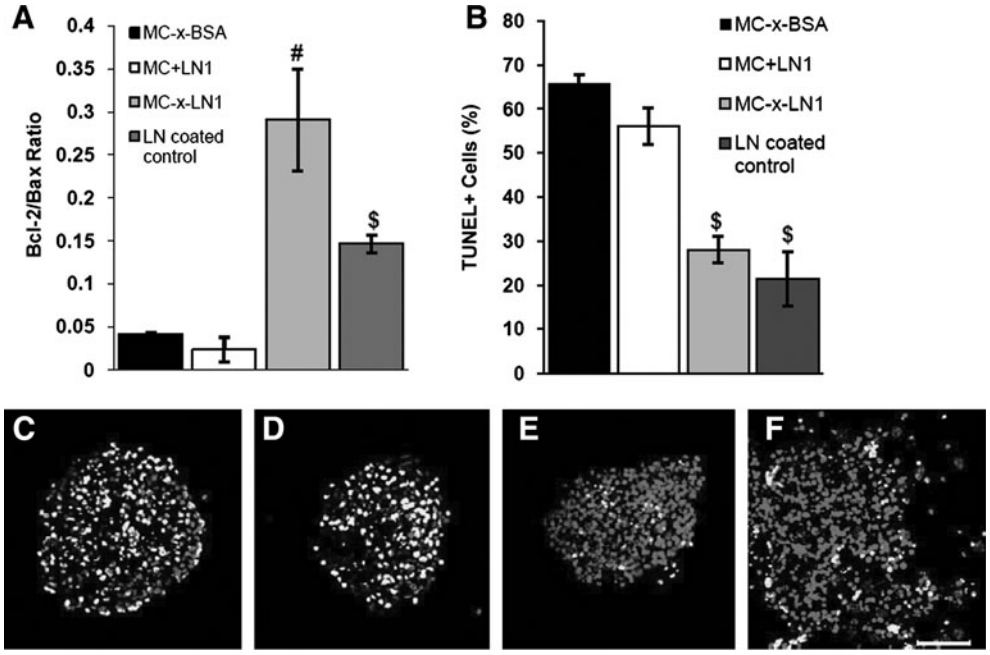

FIG. 3. Apoptosis decreased within MC-x-LN1. **(A)** At 7 days, the ratio of bcl-2 to bax, as measured by quantitative reverse transcriptase-polymerase chain reaction, showed significantly higher levels of anti-apoptotic signaling in MC-x-LN1 and LN1-coated control than in MC-x-BSA and MC+LN1. **(B)** A significantly lower percentage of $TUNEL^+$ cells were observed with MC-x-LN1 and LN1-coated than in MC-x-BSA and MC+LN1. Mean ± standard deviation, $^{\#}p < 0.05$ relative to all groups, $^{\$}p < 0.05$ relative to MC-x-BSA and MC+LN1. **(C–F)** Representative TUNEL staining of 15 μm sections of neurospheres plated within MC-x-BSA **(C)**, MC+LN1 **(D)**, MC-x-LN1 **(E)**, and on LN1-coated substrates **(F)**. Light gray = $TUNEL^+$, dark gray = Hoechst nuclei stain; scale bar = 50 μm. TUNEL, tetramethylrhodamine-dUTP nick end labeling.

outgrowth in MC-x-LN1 involves β_1 integrin receptors. NSC media supplemented with control IgG isotype antibody did not significantly alter neurite outgrowth and was therefore presented collectively with controls (Fig. 4C). Immunocytochemistry on cryosectioned cultures revealed that the projections were β-tubulin III positive, indicating a neuronal phenotype (Fig. 5). Together, these data show that while MC with traces of nontethered LN1 supports NSC migration from neurospheres, the generation of neurite projections requires an LN1-presenting matrix and β_1 integrin activity.

3D presentation of LN1 modulates differentiation

Markers of neural phenotypes were evaluated via immunocytochemistry at 7 days for neural progenitor (nestin), neuronal (β-tubulin III), astrocyte (GFAP), oligodendrocyte precursor (O4), and oligodendrocyte (NG2) lineages (Fig. 5 and Table 1). For the MC groups, NSCs were cultured in the absence of bFGF; removal of this mitogen inherently induces differentiation.[6] As expected, nestin expression diminished across all MC conditions and 2D LN1 controls (Fig. 5A, D, G, J) as compared with control NSC suspension cultures supplemented with bFGF (data not shown). There was residual nestin-positive staining in the MC groups at the neurosphere periphery and no significant differences among the MC groups ($p = 0.133$; $H = 4.562$, 2 degrees of freedom, Kruskal–Wallis ANOVA). In all MC culture conditions, an increase of GFAP expression was observed compared with bFGF controls; however, no statistical difference was detected across the MC groups (Fig. 5B, E, H) ($p = 0.604$; $H = 1.009$, 2 degrees of freedom, Kruskal–Wallis ANOVA). β-Tubulin III-positive staining significantly increased at the peripheral edges of neurospheres cultured within MC-x-LN1 (Fig. 5H) compared with MC-x-BSA ($p < 0.05$) and MC+LN1 ($p < 0.05$) ($H = 10.237$, 2 degrees of freedom, Kruskal–Wallis ANOVA), indicating that the extensions observed in the outgrowth study were of neuronal origin. NG2-positive staining was absent throughout all culture conditions. Marker O4-positive immunostaining significantly increased within MC-x-LN1 (Fig. 5I) compared with MC-x-BSA ($p < 0.05$) and MC+LN1 ($p < 0.05$) ($H = 12.639$, 2 degrees of freedom, Kruskal–Wallis ANOVA). Our findings demonstrate that engineered extracellular microenvironment surrounding the neurosphere modulates and directs the differentiation of NSCs. Specifically, while MC alone supports primarily astrocyte differentiation with minimal neuronal differentiation, the spectrum of phenotypes increased to include oligodendrocyte precursors and a more prominent neuronal population by tethering LN1 to MC.

Biomimetic extracellular environment modulates ECM production

To further examine the impact LN1 has on NSCs, we measured LN1 and FN levels and co-localization with their corresponding integrin binding receptors $\alpha_6\beta_1$ and $\alpha_5\beta_1$, respectively (Fig. 6). Antibody to the integrin subunit α_6 was used to detect $\alpha_6\beta_1$; this antibody also binds to $\alpha_6\beta_4$; however, previous reports show that β_4 integrins are minimally expressed on NSCs.[5,31] Therefore, positive α_6 stain-

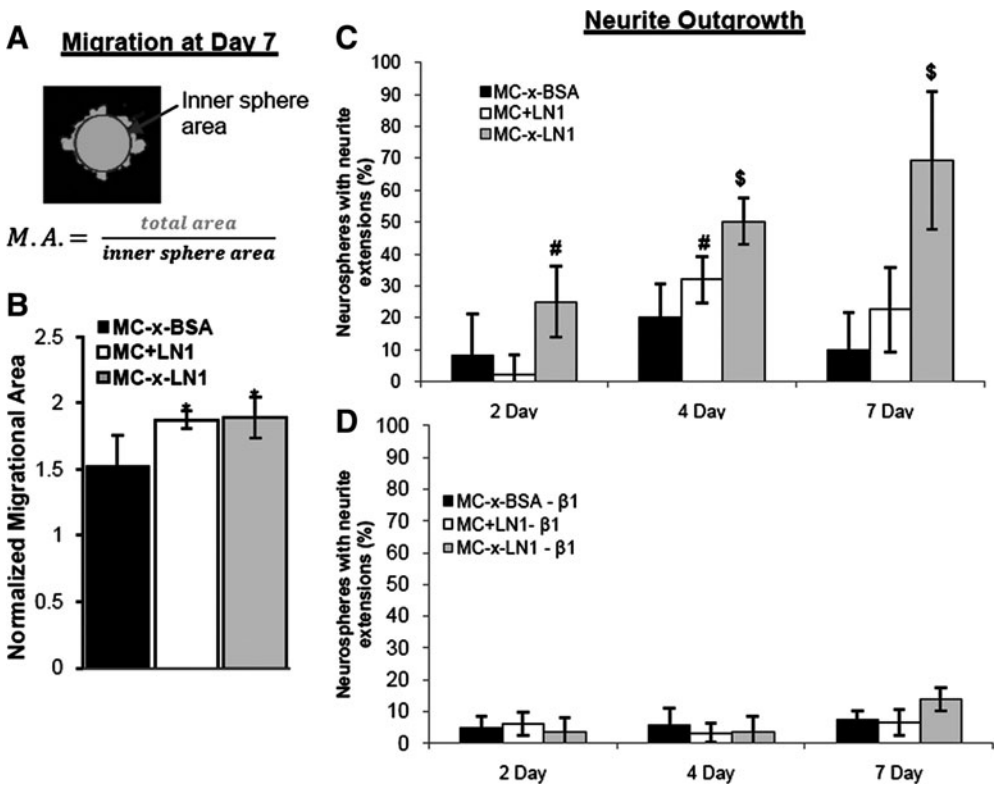

FIG. 4. MC-x-LN1 supports β_1 integrin-dependent neurite extension. **(A)** Migrational area (M.A.) was measured on confocal z-stack projects where the total spheroid area (light gray) was normalized to the inner sphere area (dark gray). **(B)** Migrations increased significantly in MC+LN1 and MC-x-LN1 compared with MC-x-BSA only at day 7. **(C)** At 4 and 7 days postplating, the percentage of viable neurospheres with neurite-like extensions was significantly higher in MC-x-LN1 than in MC-x-BSA and MC+LN1. There was no significant difference between cultures treated with control media and media supplemented with IgG isotype control. Therefore, these results were presented collectively as one group. **(D)** β_1 integrin function blocking significantly blocked neurite extension in MC-x-LN1 across all time points. Mean ± standard deviation; $^{*}p < 0.05$ relative to MC-x-BSA, $^{\$}p < 0.05$ relative to all groups; $^{\#}p < 0.05$ relative to matching β_1 integrin blocked group.

ing was considered indicative of $\alpha_6\beta_1$ integrins. NSCs plated in all MC groups stained for all probed markers, though the intensity and distribution of both ECM proteins and integrins varied across condition (Fig. 6). Area analysis for positive $\alpha_5\beta_1$ integrin signal revealed no statistical differences among MC cultures (Fig. 6D) ($F(2, 21) = 1.312$, one-way ANOVA); however, spatial patterns show positive staining at the peripheral edge of the neurospheres for MC-x-BSA and MC+LN1 compared with MC-x-LN1 (Fig. 6A–C). The area of FN-positive staining was significantly higher across neurospheres cultured in MC-x-BSA than in MC-x-LN1 (Fig. 6A–C, E) ($p < 0.05$, $F(2, 21) = 3.474$, one-way ANOVA), with dense localized FN staining across the neurosphere in MC-x-BSA. In contrast, the production of LN1 and $\alpha_6\beta_1$ in neurospheres was significantly elevated in MC-x-LN1 compared with MC-x-BSA and MC+LN1 (Fig. 6F–J) ($p > 0.05$, $F(2, 21) = 8.504$ and $F(2, 21) = 10.37$, respectively, one-way ANOVA). Further, both LN1 and $\alpha_6\beta_1$ integrins within MC-x-LN1 cultures were distributed across the entire neurosphere with enhanced intensity at the periphery. Therefore, presenting a 3D LN1 microenvironment to NSCs resulted in an upregulation of LN1 and $\alpha_6\beta_1$ integrins across the neurosphere. In contrast, lack of LN1 signaling enhanced the production of FN. Together, these data further demonstrate the influence of microenvironmental factors on the synthesis and deposition of ECM and regulation of corresponding receptors.

Discussion

Intercellular signaling involves complex cell–ECM engagements, cell–cell contacts, and cellular interactions with soluble molecules. We show that NSCs placed in a microenvironment devoid of bioadhesive signals and ECM support (i.e., MC-x-BSA) will undergo apoptosis (i.e., anoikis). The β_1 integrin family has been linked to ECM-mediated pro-survival signaling. In particular, Leone *et al.* reported increased apoptosis of NSCs derived from β_1 integrin-conditional knock-out mice.[3] Similar observations have been reported in stem cell development, where disruption of LN1 assembly in the basal lamina of embryoid bodies led to apoptosis.[1,32] Therefore, ablation of either the ECM or critical ECM receptors eliminates inherent survival mechanisms in NSCs and other developing cells.

An enhanced understanding of cell–ECM interactions will drive improved transplant therapies, as acute donor cell apoptosis posttransplantation has been linked to anoikis.[18,20,33] In many transplantation procedures, donor cells

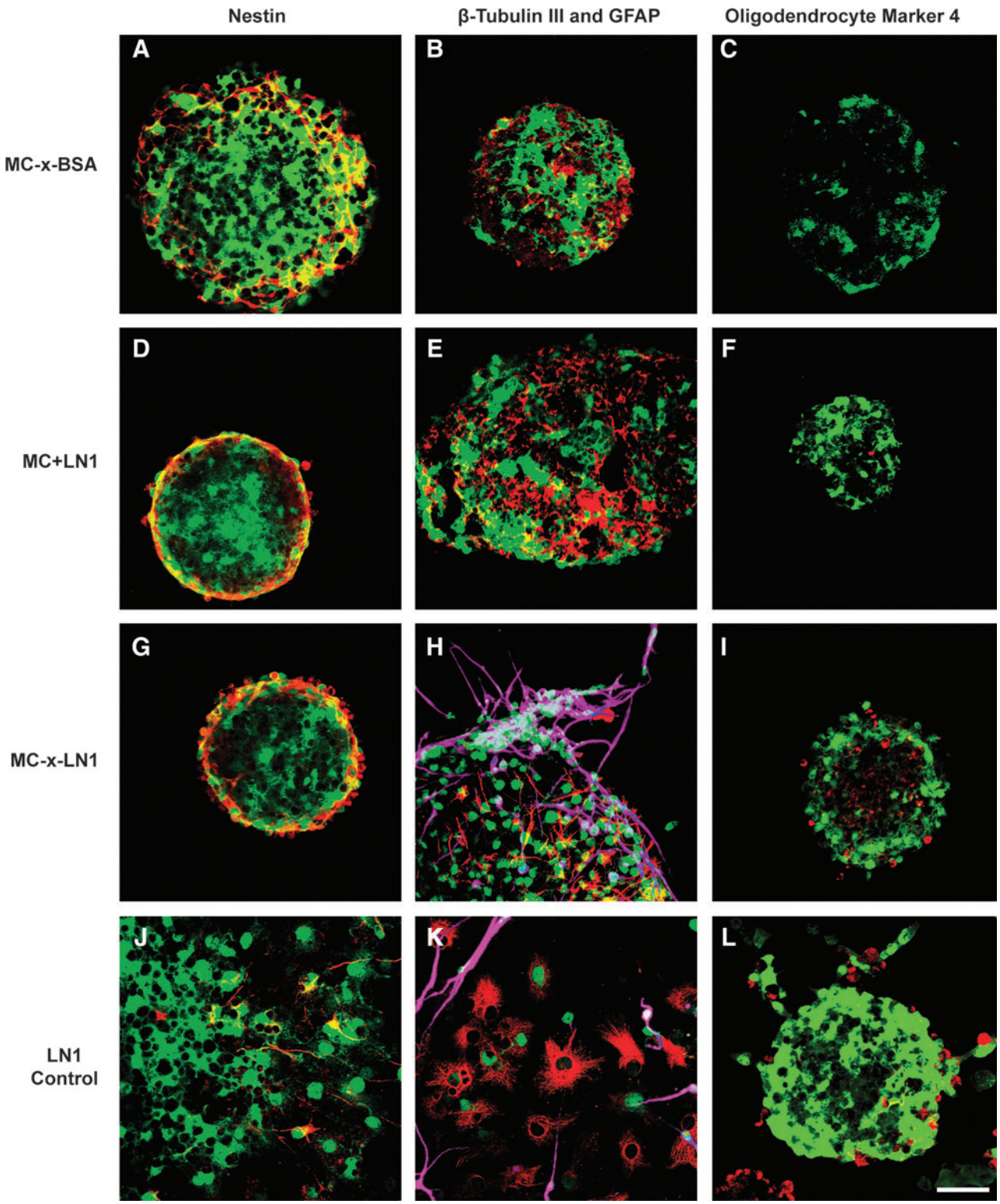

FIG. 5. Differentiation. Immunocytochemistry at 7 days revealed substantial differences in phenotype profiles within each culture condition. Representative images of MC-x-BSA **(A–C)**, MC+LN1 **(D–F)**, MC-x-LN1 **(G–I)**, and LN1-coated control **(J–L)**. Compared with basic fibroblast growth factor-treated cultures, nestin staining (red; **A, D, G, J**) diminished in all culture conditions. Increased glial fibrillary acidic protein staining (red; **B, E, H, K**) was most pronounced in MC+LN1 and LN1-coated control. β-Tubulin III (purple; **B, E, H, K**) was predominantly observed in MC-x-LN1 and LN1-coated control. O4 staining (red; **C, F, I, L**) was only observed in MC-x-LN1 and LN1-coated controls. Green = GFP on actin promoter, scale bar = 50 μm.

Table 1. Relative Scale of Phenotype Expression as Observed with Immunocytochemistry at 7 Days

	Phenotypic markers				
Group	*Nestin*	*GFAP*	*β-Tubulin III*	*O4*	*NG2*
+bFGF	+++	+	+	−	−
−bFGF	++	++	++	−	−
LN1 coated	+	+++	+++	++	−
MC-x-BSA	++	+++	+	−	−
MC+LN1	+	+++	+	−	−
MC-x-LN1	+	+++	+++[a]	+[a]	−

High, +++; moderate, ++; low, +; not detected, −.

[a]Denotes significant higher phenotype expression in MC-x-LN1 than in MC controls as determined by Kruskal–Wallis analysis of variance on ranks followed by Dunn's pairwise comparisons ($p < 0.05$).

BSA, bovine serum albumin; bFGF, basic fibroblast growth factor; LN1, laminin-1; MC, methylcellulose.

are injected in suspension form void of ECM support. In addition, transplanting cells into injured tissue exposes donor cells to deleterious molecules, further contributing to low donor cell survival.[18,34,35] Others and we hypothesize that low levels of donor cell survival are due to perturbations of pro-survival cues (e.g., cell–cell contact, cell–ECM interactions, and growth factor signaling) and inducers of necrosis and apoptosis. Marchionini *et al.* found that donor cell survival in a Parkinson's lesion model increased by preincubating transplant cell suspensions with tenascin or an antibody for cell adhesion molecule L1, possibly by reducing anoikis.[18] In the present study, we demonstrate that NSC viability was maintained when cells were cultured within MC tethered to LN1. Similar observations have been made with pancreatic islet and hepatocyte isolations, where direct plating onto LN1, FN, or collagen IV substrates decreased apoptosis.[20,33] In a previous study, we injected NSCs into mechanically injured neuronal-astrocytic cultures and found that NSCs contained high levels of caspase activity, whereas the number of caspase-positive donor cells was significantly reduced when co-delivered with MC-x-LN1.[36] Therefore, incorporating pro-survival ECM ligands within the transplant delivery vehicle may effectively improve donor cell survival through inherent survival mechanisms in the face of damaged neural tissue.

NSCs maintained in proliferative neurosphere cultures result in a heterogeneous cell population with a supporting 3D microenvironment of secreted ECM proteins and cell–cell interactions.[6] It is hypothesized that this resulting complex 3D microenvironment leads to directed differentiation and asymmetrical proliferation.[37] Therefore, alterations in the ECM deposition patterns within the spheroid may, in turn, induce corresponding phenotypic changes. Alterations in spatial phenotypic profiles due to an exogenous stimulus such as LN1 may result in modified ECM deposition. In the present study, the LN1-presenting microenvironment perturbed the spatial distribution of phenotypic markers across the neurosphere and the deposition of ECM and corresponding integrins. NSCs maintained under proliferative culture conditions (e.g., bFGF- or epidermal growth factor-supplemented medium) possess a distinct phenotypic distribution that is dependent on the spatial location within the neurosphere, where nestin-positive cells are located on the peripheral edges and more mature phenotypes (neuronal and astrocyte) are located at the center.[6] We demonstrated that introducing exogenous tethered LN1 to NSCs resulted in a higher propensity of mature phenotypic markers (neuronal, astrocytic, and oligodendrocyte) at the periphery, whereas nestin expression was reduced overall and peripherally located when present. ECM deposition and integrin receptor profiles in MC-x-LN1 were also altered compared with control cultures. Protein adsorption to MC is limited,[13] which may explain the modest responses observed in MC+LN1 compared with MC-x-LN1 as covalently tethering LN1 to MC retains LN1 within the matrix. Future studies may investigate a potential LN concentration effect on differentiation and protein production. Previous studies reported that neurospheres maintained with mitogens (bFGF or epidermal growth factor) exhibit LN1 production predominantly in the center.[6] In contrast, we demonstrated that an LN1 microenvironment augmented production of LN1 and $\alpha_6\beta_1$ integrins across the spheroid, with the most intensity at the periphery. The corresponding phenotype pattern indicated that LN1 production might be of either neuronal or astrocytic origin as both cell types have been shown to produce LN1.[38] Therefore, deposition of LN1 may further push neuronal differentiation. We established that, by altering the exogenous microenvironment of NSC cultures, the phenotype and the ECM and integrin profiles are modified. Questions still remain as to whether phenotypic changes occurred before ECM modifications or vice versa.

An alternative approach to generating a biomimetic LN-based hydrogel is to incorporate known bioactive peptide sequences. This approach has proven fruitful in increasing adhesion, viability, and differentiation of NSCs within a collagen gel[39] and self-assembled nanofibers.[40] Additionally, the mechanical properties of hydrogels also influence stem cell behavior.[41] Notably, pluripotent mesenchymal stem cells plated on substrates of differing rigidities expressed phenotypic markers of tissues with similar mechanical properties; soft substrates (E $\sim$0.1–1 kPa) yielded cell populations expressing neuronal markers.[41] Recent studies with NSCs in alginate,[42] poly(ethylene glycol) (PEG)/poly(L-lysine),[43] functionalized chitosan,[44] hyaluronic acid,[45] and PEG-acrylamide[46] hydrogels reported an increase in NSC proliferation, migration, and/or neuronal differentiation in softer hydrogel formulations (G* $\sim$0.1–1 kPa; E $\sim$1–7 kPa) compared with stiffer formulations. The MC hydrogels used in our studies were formulated to have a complex modulus of $\sim$0.45 kPa (Supplementary Fig. S1, available online at www.liebertonline.com) within the aforementioned range to promote neural differentiation. Nevertheless, each of the aforementioned mechanical studies required incorporation of a bioactive molecule to ensure cell activity. Therefore, in this study, we focused on how the presence or absence of LN1 affected NSC fate within a mechanically favorable environment.

Increasing in complexity, 3D hydrogels can be used to evaluate the combination of bioadhesive and soluble mitogenic factors. For example, NSCs suspended within a

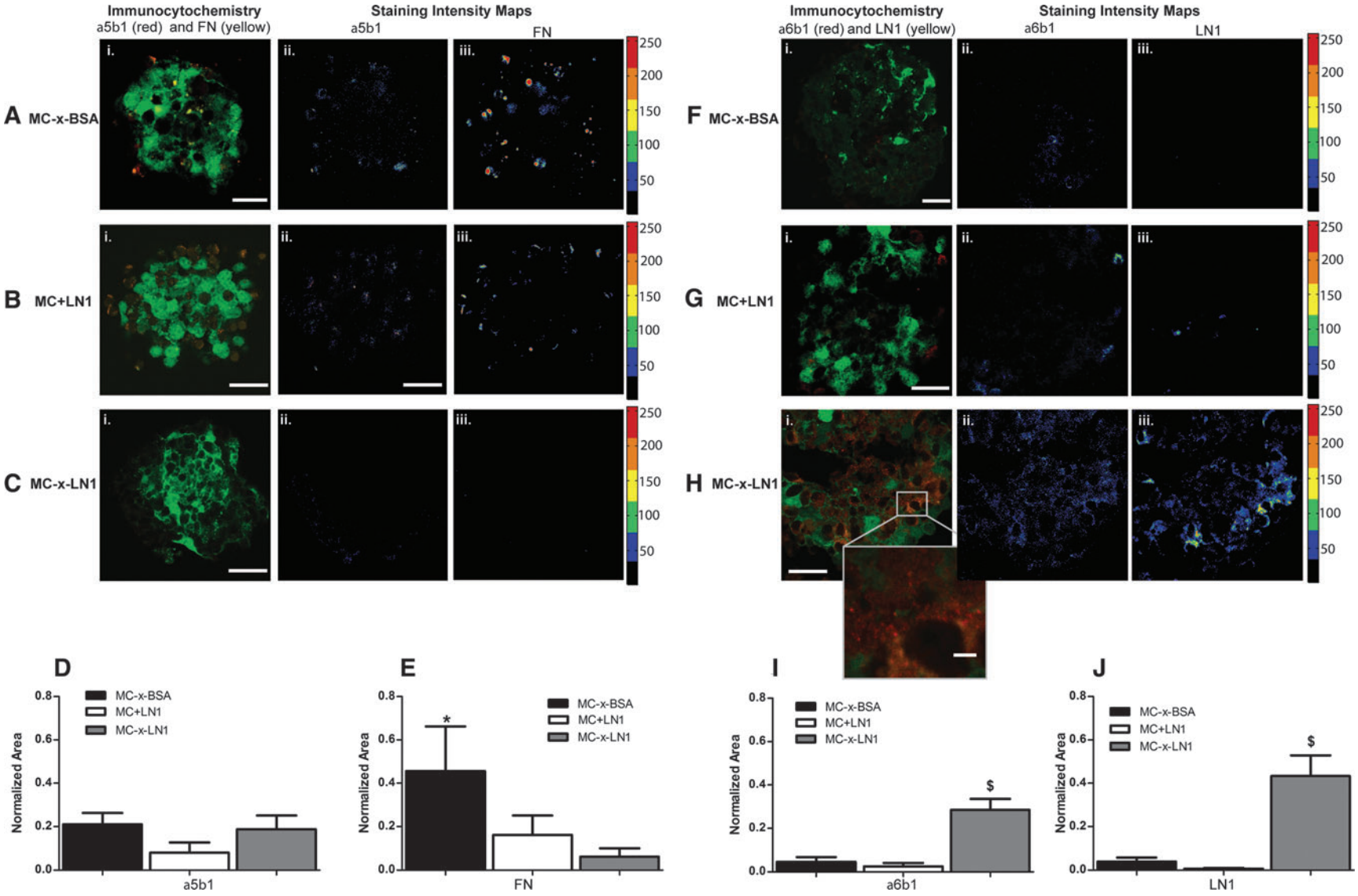

FIG. 6. Altered extracellular matrix and integrin production within MC-x-LN1- Immunocytochemistry at 7 days revealed alterations in the extracellular matrix and integrin production that were dependent on culture condition. FN (yellow) and integrin $\alpha_5\beta_1$ integrin (red) staining with MC-x-BSA **(Ai)**, MC+LN1 **(Bi)**, and MC-x-LN1 **(Ci)** cultures with corresponding signal intensity maps for each immunolabel (**Aii** to **Cii**, $\alpha_5\beta_1$ integrin intensity maps; **Aiii** to **Ciii**, FN intensity maps). LN1 (yellow) and $\alpha_6\beta_1$ integrin (red) staining on MC-x-BSA **(Fi)**, MC+LN1 **(Gi)**, and MC-x-LN1 **(Hi)** cultures with corresponding signal intensity maps for each immunolabel (**Fii** to **Hii**, $\alpha_6\beta_1$ integrin intensity maps; **Fiii** to **Hiii**, LN1 intensity maps). Green = GFP on actin promoter, scale bar = 20 μm except where noted. Normalized area of positive immunostaining for each respective probe: $\alpha_5\beta_1$ integrin **(D)**, FN **(E)**, $\alpha_6\beta_1$ integrin **(I)**, and LN1 **(J)**. Bar graphs represent mean ± standard error; $^{*}p < 0.05$ relative to MC-x-LN1, $^{\$}p < 0.05$ relative all groups. FN, fibronectin.

poly(ethylene glycol)/poly(lactic acid) (PEG-PLA) hydrogel with collagen I and bFGF exhibited increased proliferation, survival, and neuronal expression compared with a PEG-PLA hydrogel with either collagen I or bFGF alone.[8] Comparatively, we observed a markedly altered phenotypic profile in the presence of tethered LN1 without exogenous mitogenic support. Future investigations that add exogenous growth factors to MC-x-LN1 would lend insight into any synergistic or antagonistic signaling.

In conclusion, by controlling the presentation LN1 within a novel engineered 3D scaffold, we evaluated the influence of cell–ECM interactions on NSC fate. This engineered MC-x-LN1 hydrogel is advantageous over current systems due to the minimal nonspecific protein adsorption to MC and the potential to translate to clinical modalities such as cell transplantation. We observed a significant improvement of NSC survival using the tethered MC-x-LN1 scaffold and profound enhancement of neurite outgrowth and differentiation compared with MC matrices void of ECM signals. We acknowledge that NSC development is directed by many complex signals in addition to cell–ECM interactions. This controlled matrix provides a novel platform in which additional stimuli can be introduced to evaluate multiple stimuli on NSCs for improved therapeutic approaches that require NSC control.

Acknowledgments

The project was partially funded by an NIH NRSA award (SES; F31 NS054527), NSF EEC-9731643 (M.C.L.), NIH EB001014 (M.C.L.), and NIH EB004496 (A.J.G.). The authors thank Tim Petrie for technical assistance with the antibody blocking studies. We also thank M. Okabe at Osaka University for the generous gift of the GFP mice. We acknowledge Scott Medway and Vishnu Ambur for assisting with the image quantification.

Disclosure Statement

No competing financial interests exist for any of the authors.

References

1. Li, S., Harrison, D., Carbonetto, S., Fassler, R., Smyth, N., Edgar, D., and Yurchenco, P.D. Matrix assembly, regulation, and survival functions of laminin and its receptors in embryonic stem cell differentiation. J Cell Biol **157,** 1279, 2002.
2. Reynolds, B.A., Tetzlaff, W., and Weiss, S. A multipotent EGF-responsive striatal embryonic progenitor cell produces neurons and astrocytes. J Neurosci **12,** 4565, 1992.
3. Leone, D.P., Relvas, J.B., Campos, L.S., Hemmi, S., Brakebusch, C., Fassle, R., Ffrench-Constant, C., and Suter U. Regulation of neural progenitor proliferation and survival by b1 integrins. J Cell Sci **118,** 2589, 2005.
4. Tate, M.C., Garcia, A.J., Keselowsky, B.G., Schumm, M.A., Archer, D.R., and LaPlaca, M.C. Specific beta-1 integrins mediate adhesion, migration, and differentiation of neural progenitors derived from the embryonic striatum. Mol Cell Neurosci **27,** 22, 2004.
5. Jacques, T.S., Relvas, J.B., Nishimura, S., Pytela, R., Edwards, G.M., Streuli, C.H., and Ffrench-Constant, C. Neural precursor cell chain migration and division are regulated through different beta 1 integrins. Development **125,** 3167, 1998.
6. Campos, L.S., Leone, D.P., Relvas, J.B., Brakebusch, C., Fassler, R., Suter, U., and Ffrench-Constant, C. Beta1 integrins activate a MAPK signalling pathway in neural stem cells that contributes to their maintenance. Development **131,** 3433, 2004.
7. Kerever, A., Schnack, J., Vellinga, D., Ichikawa, N., Moon, C., Arikawa-Hirasawa, E., Efird, J.T., and Mercier, F. Novel extracellular matrix structures in the neural stem cell niche capture the neurogenic factor FGF-2 from the extracellular milieu. Stem Cells **25,** 2146, 2007.
8. Mahoney, M.J., and Anseth, K.S. Contrasting effects of collagen and bFGF-2 on neural cell function in degradable synthetic PEG hydrogels. J Biomed Mater Res A **81,** 269, 2007.
9. Saha, K., Irwin, E.F., Kozhukh, J., Schaffer, D.V., and Healy, K.E. Biomimetic interfacial interpenetrating polymer networks control neural stem cell behavior. J Biomed Mater Res A **81,** 240, 2007.
10. Nakajima, M., Ishimuro, T., Kato, K., Ko, I.K., Hirata, I., Arima, Y., and Iwata, H. Combinatorial protein display for the cell-based screening of biomaterials that direct neural stem cell differentiation. Biomaterials **28,** 1040, 2007.
11. Cukierman, E., Pankov, R., Stevens, D.R., and Yamada, K.M. Taking cell-matrix adhesions to the third dimension. Science **294,** 1708, 2001.
12. Friedl, P., and Brocker, E.B. The biology of cell locomotion within three-dimensional extracellular matrix. Cell Mol Life Sci **57,** 41, 2000.
13. Tate, M.C., Shear, D.A., Hoffman, S.W., Stein, D.G., and LaPlaca, M.C. Biocompatibility of methylcellulose-based constructs designed for intracerebral gelation following experimental traumatic brain injury. Biomaterials **22,** 1113, 2001.
14. Stabenfeldt, S.E., Garcia, A.J., and LaPlaca, M.C. Thermoreversible laminin-functionalized hydrogel for neural tissue engineering. J Biomed Mater Res A **77A,** 718, 2006.
15. Gupta, D., Tator, C.H., and Shoichet, M.S. Fast-gelling injectable blend of hyaluronan and methylcellulose for intrathecal, localized delivery to the injured spinal cord. Biomaterials **27,** 2370, 2006.
16. Wells, M.R., Kraus, K., Batter, D.K., Blunt, D.G., Weremowitz, J., Lynch, S.E., Antoniades, H.N., and Hansson, H.A. Gel matrix vehicles for growth factor application in nerve gap injuries repaired with tubes: a comparison of biomatrix, collagen, and methylcellulose. Exp Neurol **146,** 395, 1997.
17. Bakshi, A., Keck, C.A., Koshkin, V.S., LeBold, D.G., Siman, R., Snyder, E.Y., and McIntosh, T.K. Caspase-mediated cell death predominates following engraftment of neural progenitor cells into traumatically injured rat brain. Brain Res **1065,** 8, 2005.
18. Marchionini, D.M., Collier, T.J., Camargo, M., McGuire, S., Pitzer, M., and Sortwell, C.E. Interference with anoikis-induced cell death of dopamine neurons: implications for augmenting embryonic graft survival in a rat model of Parkinson's disease. J Comp Neurol **464,** 172, 2003.
19. Tate, M.C., Shear, D.A., Hoffman, S.W., Stein, D.G., Archer, D.R., and LaPlaca, M.C. Fibronectin promotes survival and migration of primary neural stem cells transplanted into the traumatically injured mouse brain. Cell Transplant **11,** 283, 2002.

20. Pinkse, G.G., Bouwman, W.P., Jiawan-Lalai, R., Terpstra, O.T., Bruijn, J.A., and de Heer, E. Integrin signaling via RGD peptides and anti-beta1 antibodies confers resistance to apoptosis in islets of Langerhans. Diabetes **55,** 312, 2006.
21. Tate, C.C., Shear, D.A., Tate, M.C., Archer, D.R., Stein, D.G., and LaPlaca, M.C. Laminin and fibronectin scaffolds enhance neural stem cell transplantation into the injured brain. J Tissue Eng Regen Med **3,** 208, 2009.
22. Okabe, S., ForsbergNilsson, K., Spiro, A.C., Segal, M., and McKay, R.D.G. Development of neuronal precursor cells and functional postmitotic neurons from embryonic stem cells *in vitro*. Mech Dev **59,** 89, 1996.
23. Kobayashi, K., Huang, C.I., and Lodge, T.P. Thermoreversible gelation of aqueous methylcellulose solutions. Macromolecules **32,** 7070, 1999.
24. Decker, T., and Lohmann-Matthes, M.L. A quick and simple method for the quantitation of lactate dehydrogenase release in measurements of cellular cytotoxicity and tumor necrosis factor (TNF) activity. J Immunol Methods **115,** 61, 1988.
25. Watanabe, K., Nakamura, M., Okano, H., and Toyama, Y. Establishment of three-dimensional culture of neural stem/progenitor cells in collagen Type-1 Gel. Restor Neurol Neurosci **25,** 109, 2007.
26. Byers, B.A., Pavlath, G.K., Murphy, T.J., Karsenty, G., and Garcia, A.J. Cell-type-dependent up-regulation of *in vitro* mineralization after overexpression of the osteoblast-specific transcription factor Runx2/Cbfa1. J Bone Miner Res **17,** 1931, 2002.
27. Boley, S.E., Wong, V.A., French, J.E., and Recio, L. p53 heterozygosity alters the mRNA expression of p53 target genes in the bone marrow in response to inhaled benzene. Toxicol Sci **66,** 209, 2002.
28. Brazel, C.Y., Limke, T.L., Osborne, J.K., Miura, T., Cai, J., Pevny, L., and Rao, M.S. Sox2 expression defines a heterogeneous population of neurosphere-forming cells in the adult murine brain. Aging Cell **4,** 197, 2005.
29. Williams, C.M., Engler, A.J., Slone, R.D., Galante, L.L., and Schwarzbauer, J.E. Fibronectin expression modulates mammary epithelial cell proliferation during acinar differentiation. Cancer Res **68,** 3185, 2008.
30. Chao, D.T., and Korsmeyer, S.J. BCL-2 family: regulators of cell death. Annu Rev Immunol **16,** 395, 1998.
31. Hall, P.E., Lathia, J.D., Miller, N.G., Caldwell, M.A., and Ffrench-Constant, C. Integrins are markers of human neural stem cells. Stem Cells **24,** 2078, 2006.
32. Miner, J.H., Li, C., Mudd, J.L., Go, G., and Sutherland, A.E. Compositional and structural requirements for laminin and basement membranes during mouse embryo implantation and gastrulation. Development **131,** 2247, 2004.
33. Pinkse, G.G., Voorhoeve, M.P., Noteborn, M., Terpstra, O.T., Bruijn, J.A., and De Heer, E. Hepatocyte survival depends on beta1-integrin-mediated attachment of hepatocytes to hepatic extracellular matrix. Liver Int **24,** 218, 2004.
34. Molcanyi, M., Riess, P., Bentz, K., Maegele, M., Hescheler, J., Schafke, B., Trapp, T., Neugebauer, E., Klug, N., and Schafer, U. Trauma-associated inflammatory response impairs embryonic stem cell survival and integration after implantation into injured rat brain. J Neurotrauma **24,** 625, 2007.
35. Boockvar, J.A., Schouten, J., Royo, N., Millard, M., Spangler, Z., Castelbuono, D., Snyder, E., O'Rourke, D., and McIntosh, T. Experimental traumatic brain injury modulates the survival, migration, and terminal phenotype of transplanted epidermal growth factor receptor-activated neural stem cells. Neurosurgery **56,** 163, 2005.
36. Cullen, D.K., Stabenfeldt, S.E., Simon, C.M., Tate, C.C., and Laplaca, M.C. *In vitro* neural injury model for optimization of tissue-engineered constructs. J Neurosci Res **85,** 3642, 2007.
37. Campos, L.S. Neurospheres: insights into neural stem cell biology. J Neurosci Res **78,** 761, 2004.
38. Liesi, P., Fried, G., and Stewart, R.R. Neurons and glial cells of the embryonic human brain and spinal cord express multiple and distinct isoforms of laminin. J Neurosci Res **64,** 144, 2001.
39. Hiraoka, M., Kato, K., Nakaji-Hirabayashi, T., and Iwata, H. Enhanced survival of neural cells embedded in hydrogels composed of collagen and laminin-derived cell adhesive peptide. Bioconjug Chem **20,** 976, 2009.
40. Silva, G.A., Czeisler, C., Niece, K.L., Beniash, E., Harrington, D.A., Kessler, J.A., and Stupp, S.I. Selective differentiation of neural progenitor cells by high-epitope density nanofibers. Science **303,** 1352, 2004.
41. Engler, A.J., Sen, S., Sweeney, H.L., and Discher, D.E. Matrix elasticity directs stem cell lineage specification. Cell **126,** 677, 2006.
42. Banerjee, A., Arha, M., Choudhary, S., Ashton, R.S., Bhatia, S.R., Schaffer, D.V., and Kane, R.S. The influence of hydrogel modulus on the proliferation and differentiation of encapsulated neural stem cells. Biomaterials **30,** 4695, 2009.
43. Hynes, S.R., Rauch, M.F., Bertram, J.P., and Lavik, E.B. A library of tunable poly(ethylene glycol)/poly(L-lysine) hydrogels to investigate the material cues that influence neural stem cell differentiation. J Biomed Mater Res A **89A,** 499, 2009.
44. Leipzig, N.D., Xu, C., Zahir, T., and Shoichet, M.S. Functional immobilization of interferon-gamma induces neuronal differentiation of neural stem cells. J Biomed Mater Res A **93,** 625, 2010.
45. Seidlits, S.K., Khaing, Z.Z., Petersen, R.R., Nickels, J.D., Vanscoy, J.E., Shear, J.B., and Schmidt, C.E. The effects of hyaluronic acid hydrogels with tunable mechanical properties on neural progenitor cell differentiation. Biomaterials **31,** 3930, 2010.
46. Saha, K., Keung, A.J., Irwin, E.F., Li, Y., Little, L., Schaffer, D.V., and Healy, K.E. Substrate modulus directs neural stem cell behavior. Biophys J **95,** 4426, 2008.

Address correspondence to:
Michelle C. LaPlaca, Ph.D.
Laboratory for Neuroengineering
Coulter Department of Biomedical Engineering
Petit Institute for Bioengineering and Bioscience
Georgia Institute of Technology
Emory University
313 Ferst Drive
Atlanta, GA 30332-0535

E-mail: michelle.laplaca@bme.gatech.edu

Received: December 29, 2009
Accepted: July 19, 2010
Online Publication Date: September 27, 2010